Analytical Methods

ROYAL SOCIETY OF CHEMISTRY

PAPER

View Article Online
View Journal | View Issue

Cite this: *Anal. Methods*, 2022, **14**, 241

Investigating protein diffusivities in diluted hyaluronic acid solutions using dynamic light scattering

Hao Lou *[ab] and Michael J. Hageman*[ab]

This study aimed to investigate the diffusivities of lysozyme (LYS), ovalbumin (OVA), and hyaluronic acid (HA) in buffered solvents using dynamic light scattering (DLS). For protein/solvent and HA/solvent binary systems, the diffusion coefficients of protein or HA were obtained from autocorrelation function (ACF) curve fitting. Whereas, for protein/HA/solvent ternary systems, the two eigenvalues of the mutual diffusion coefficient matrix were obtained from ACF curve fitting. The results of binary systems showed that at low ionic strength, the diffusion coefficients of protein and HA increased linearly with concentration; at high ionic strength, the diffusion coefficients of OVA and LYS were independent on protein concentration; for HA, the positive linear relationship between diffusion coefficient and concentration existed at high and low ionic strengths, but the slope at high ionic strength was smaller compared to that at low ionic strength. For OVA/HA/solvent ternary systems, the sum of two eigenvalues (D^1_{DLS} + D^2_{DLS}) was slightly smaller compared to (D_{OVA} + D_{HA}), where D_{OVA} and D_{HA} were the diffusion coefficients in their binary systems. On the contrary, for LYS/HA/solvent ternary systems, (D^1_{DLS} + D^2_{DLS}) were significantly smaller than (D_{LYS} + D_{HA}) and the diffusion coefficients in binary and ternary systems exhibited an opposite trend with respect to ionic strength change. The DLS and MD simulation results indicated strong attractive intermolecular interaction existed between LYS and HA molecules, especially at low ionic strength. By using DLS, it was possible to characterize the diffusion coefficients of diluted protein/HA binary and ternary systems.

Received 28th October 2021
Accepted 25th December 2021

DOI: 10.1039/d1ay01832a

rsc.li/methods

1. Introduction

Hyaluronic acid (HA) is a linear, un-branched polysaccharide that is composed of repeatable disaccharide monomers of D-glucuronic acid (GlcNAc) and *N*-acetyl-D-glucosamine (GlcA) linked *via* a β-1,4 glycosidic bond. For human beings and other vertebrates, HA exists widely and ubiquitously in the extracellular matrix (ECM), and its distribution varies on concentration and molecular weight throughout different species, organs, and tissues.[1–3] While delivering peptide and protein based biotherapeutics *via* different routes such as subcutaneous (SC), ocular, and intratumor routes, HA slows down the migration of biotherapeutics inside the ECM, because HA is highly viscous and can act as a molecular sieve.[4] Further, because GlcA's carboxylic acid group is negatively charged at physiological pH (*e.g.*, 7.4), HA tends to interact with some positively charged biotherapeutics and even lead to the formation of insoluble complexes.[5] Therefore, an *in vitro* method that can characterize the diffusivity of biotherapeutics in HA solution is pivotal and would help to better understand biotherapeutic transport inside the ECM *in vivo*.

The dynamic light scattering (DLS) technique offers a solution. Based on light intensity fluctuation caused by the Brownian motion of nano-colloids, DLS generates an autocorrelation function (ACF) *versus* time, and the decay constant(s) of this ACF is directly associated with the mutual diffusion coefficient(s).[6,7] For binary systems, the diffusion coefficient (D_{DLS}) obtained from ACF curve fitting aligns with the diffusion coefficient defined by the Fick's first law.[6,7]

$$J = -D\nabla C \tag{1}$$

For ternary systems, two diffusion coefficients (D^1_{DLS} and D^2_{DLS}) can be obtained from ACF curve fitting. However, according to the extended Fick's first law, diffusion is described by a diffusion coefficient matrix containing four diffusion coefficients, as shown in eqn(2) and (3):

$$J_1 = -D_{11}\nabla C_1 - D_{12}\nabla C_2 \tag{2}$$

$$J_2 = -D_{21}\nabla C_1 - D_{22}\nabla C_2 \tag{3}$$

where J_1 and J_2 are the fluxes of two solutes, D_{11} and D_{22} are the main diffusion coefficients at their own concentration gradients, whereas D_{12} and D_{21} are the cross-diffusion coefficients.

[a]*Department of Pharmaceutical Chemistry, University of Kansas, Lawrence, KS, 66047, USA. E-mail: lou0@ku.edu; mhageman@ku.edu*

[b]*Biopharmaceutical Innovation and Optimization Center, University of Kansas, Lawrence, KS, 66047, USA*

It is reported that the two diffusion coefficients obtained from DLS (D^1_{DLS} and D^2_{DLS}) coincide with the two eigenvalues $D\begin{pmatrix}2\\1\end{pmatrix}$ of the mutual diffusion coefficient matrix (shown in eqn (4)):[8]

$$D\begin{pmatrix}2\\1\end{pmatrix} = \frac{D_{11} + D_{22} \pm (D_{22} - D_{11})\sqrt{1 + \left[4D_{12}D_{21}\Big/(D_{22} - D_{11})^2\right]}}{2} \quad (4)$$

If ternary systems are diluted and consist of non-ionic, low molecular weight molecules, using some theoretical computation/simulation methods, the DLS ACF might be further deconvoluted to attain D_{11}, D_{22}, D_{12}, and D_{21}, separately, and these diffusion coefficients are consistent with those measured by other techniques such as Taylor dispersion.[8–10] However, to the best of our knowledge, to date, there is a lack of deconvolution methods that can apply to the complex ternary systems such as the systems in the present study, where both protein and HA are macromolecules with un-uniform surface charge density and strong intermolecular interactions. Nevertheless, the eigenvalues can still reveal valuable information about molecule diffusivity. Also, using DLS for diffusivity characterization possesses lots of advantages such as accuracy, convenience, fast measurement, high resolution, and small sample size.

This study aims to characterize protein/HA diffusivities in a series of diluted binary systems (*e.g.*, protein/solvent, HA/solvent) and ternary systems (*e.g.*, protein/HA/solvent) using DLS. The effect of various factors such as concentration, ionic strength, and temperature on macromolecule diffusivity is thoroughly explored. In addition, compared to the systems investigated in the present study, characterizing molecule diffusivities in a physiologically relevant system(s) is more challenging since (1) ECM is a mixture containing multiple components; and (2) for some tissues and organs, the HA level inside ECM is higher than the regime investigated in this study. In general, concentrated systems are more likely to experience some issues such as multiple scattering.[11] Hence, the proposed DLS method might be only capable to analyze diluted binary and ternary systems. Nevertheless, the knowledge gained in this work may help to further understand protein diffusion in more complicated systems such as physiologically relevant conditions.

2. Materials and methods

2.1. Material and sample preparation

Lysozyme (LYS) from chicken egg white (lyophilized powder, MW 14.3 kDa), ovalbumin (OVA) from chicken egg white (lyophilized powder, MW 44.3 kDa), sodium phosphate dibasic, and sodium phosphate monobasic were purchased from Sigma Aldrich (MO, USA). Sodium hyaluronate (HA) (average MW 1.5 MDa) was purchased from Lifecore Biomedical LLC (MN, USA). Gibco phosphate buffered saline (PBS) (pH 7.4, 1×) was purchased from ThermoFisher (MA, USA). All solvents used in this study were of analytical grade.

A series of buffered solvent systems with different total ionic strengths were prepared by mixing 10 mM phosphate buffer (pH 7.4, total ionic strength: 26 mM) and PBS 1× (pH 7.4, total ionic strength: approximately 163 mM) with preset ratios. Each sample was prepared by weighing and dissolving HA and/or protein powders in buffered solvents, followed by the filtration through 0.22 μm filters (Whatman plc, Maidstone, UK).

2.2. DLS measurements

Diffusivity measurements were carried out using a Malvern Zetasizer® (Malvern Instruments, Malvern, UK), equipped with a 633 nm laser at 173° scattering angle with the backscatter detection only. Samples were evaluated at four temperatures: 25, 30, 34, and 37 °C. Prior to each run, 1 mL of freshly prepared sample was loaded into an ultramicro UV cuvette, followed by the capping with an LDPE plug. The loaded sample was pre-equilibrated for 120 seconds, and then measured at controlled temperatures. For each experimental condition/sample combination, a total of nine replicates ($n = 9$) were performed.

2.3. ACF curve fitting algorithms

DLS provides a normalized second-order ACF intensity curve ($G^2(t) - 1$) *versus* time (t). Since (1) light intensities were predominantly contributed by macromolecules such as HA and proteins rather than small ions/molecules; (2) cross-diffusion coefficients caused by small ions should be much less notable compared to those caused by macromolecules, it was reasonable to treat solvent as one component, HA/solvent and protein/solvent as a pseudo-binary system, and HA/protein/solvent as a pseudo-ternary system. The ACF curve was fit by nonlinear regression based on the 'Levenberg–Marquardt' algorithm using the following equations.

For LYS/solvent binary systems, the ACF curve was fit by eqn (5),

$$G^2(t) - 1 = (I_f \exp(-t/\tau_f) + I_s \exp(-t/\tau_{se}))^2 \quad (5)$$

where I_f and I_s were the intensities of the fast and slow relaxation modes, τ_f was the characteristic decay time related to diffusion, and τ_{se} was the characteristic decay time associated with slow relaxation such as molecular moiety relaxation and/or disengagement of side chains of molecules, molecule entanglement, as well as some imperfect signal collection if there was any.[12,13] For OVA/solvent and HA/solvent systems, the ACF curve was fit by eqn (6),

$$G^2(t) - 1 = (I_f \exp(-t/\tau_f) + I_s \exp(-t/\tau_{se})^{\beta})^2 \quad (6)$$

Compared to eqn (5), a new term β, used as a correction factor within the range of (0,1) to define the width and shape of the slow relaxation modes, was added for better curve fitting. Noteworthy, the size exclusion chromatograph data from previous literature[14] and our preliminary data found that, by nature, OVA molecules prepared by dissolving lyophilized powder stayed in a monomeric form and a dimeric form

approximately with a ratio of 5 : 1 by weight. However, the DLS signals of these two forms were not separated out and were still expressed by one exponential term in eqn (6). Therefore, in this study, DLS measured the diffusion coefficient of all OVA forms as a whole.

For HA/protein/solvent ternary systems, ACF was fit by three exponential terms, as shown in eqn (7),

$$G^2(t) - 1 = (I_{f1}\exp(-t/\tau_{f1}) + I_{f2}\exp(-t/\tau_{f2}) + I_s\exp(-t/\tau_{se})^{\beta})^2 \quad (7)$$

where the former two terms were related to the eigenvalues of the mutual diffusion coefficient matrix for HA and protein, and the third term was associated with slow relaxation and imperfect signal collection.

2.4. Diffusion coefficient calculation

Knowing the value of τ_f, D_{DLS} was determined by the equation $D_{DLS} = 1/q^2\tau_f$, with $q = \frac{4\pi n_0}{\lambda}\sin\left(\frac{\theta}{2}\right)$, where n_0 was solvent refractive index, λ was the wavelength of incident light, and θ was the angle of incident light.[6] For binary systems, D_{DLS} was the mutual diffusion coefficient of protein or HA. By contrary, for ternary systems, the sum of two eigenvalues (D^1_{DLS} + D^2_{DLS}), which was equivalent to (D_{11} + D_{22}) (this relation can be derived from eqn (4)), was chosen for further data analysis and discussion, since the individual diffusion coefficients could not be isolated using the current methodologies.

2.5. Molecular dynamic simulation

To further understand the effect of ionic strength on LYS–HA intermolecular interaction, molecular dynamic (MD) simulation was performed using GROMACS, version 2020.3.[15] Due to the computation capacity, this simulation was carried out in a small system that was not a strict duplication of the actual ternary systems of the present study. The MD simulation parameters and procedures were listed as follows. The OPLS-AA/L all-atom force field was applied. The topology of LYS was built based on the published lysozyme structure with PDB code 1AKI.[16] The topology of HA monomer (molecular charge: −1) was generated using LigParGen server.[17,18] Water was modeled

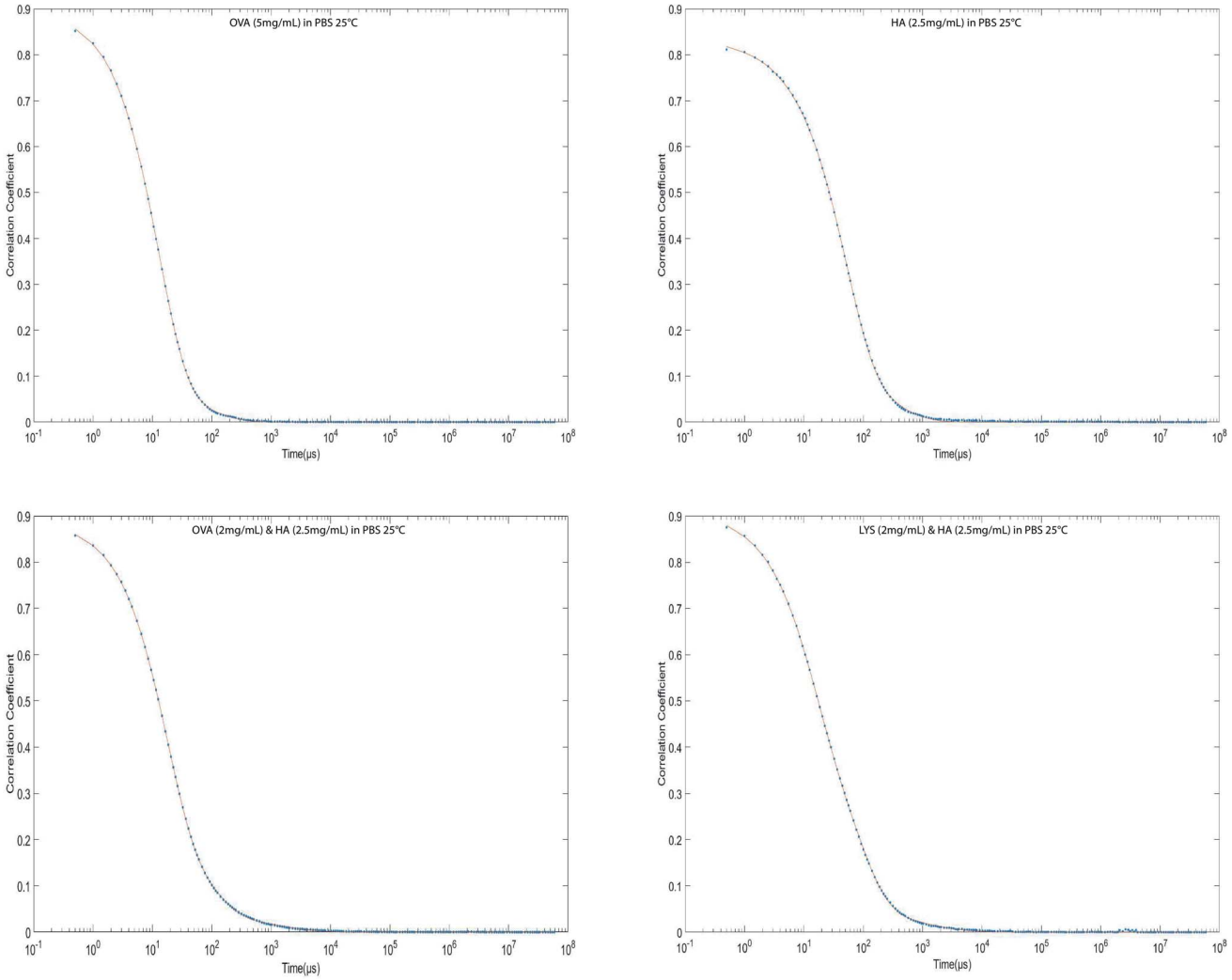

Fig. 1 Four examples of the autocorrelation functions.

using SPC/E water model. At the initial state, 1 LYS molecule and 8 HA monomer molecules were randomly inserted into a $(7.01\ \text{nm})^3$ cubic box filled with around 10^4 water molecules. To simulate different ionic strengths, according to our calculation, 45 mM was correspondent to 9 Na^+ and 9 Cl^- ions randomly distributed in the box, 80 mM was correspondent to 17 Na^+ and 17 Cl^- ions, and 150 mM was correspondent to 31 Na^+ and 31 Cl^- ions. Next, the system was relaxed through energy minimization and equilibrated under NVT and NPT conditions. The full MD simulation was conducted for 10 ps with a 2 fs time step. For short-range electrostatics and short-range van der Waals interactions, 1 nm was used as the cutoff distance. For long-range electrostatic interactions, particle-mesh-Ewald (PME) method was used. V-rescale method was chosen for temperature coupling with 0.1 ps time constant and 307 K reference temperature. Parrinello–Rahman method was chosen for pressure coupling with 2 ps time constant, 1 bar reference pressure, and 4.5×10^{-5} per bar compressibility. To analyze LYS–HA interaction, LYS and HA were grouped and the simulation trajectory was re-ran to calculate the interaction energy.

3. Results and discussion

3.1. Autocorrelation functions

Fig. 1 presented four examples of the curve fitting of the ACFs for both the binary and the ternary systems. As shown, the equations with two exponential terms could accurately fit the ACFs of the binary systems, and the equations with three exponential terms could fit the ACFs of the ternary systems. It was worth pointing out that the exponential term representing the slow relaxation mode could significantly improve the curve fitting of the experimental data. For the ACFs of the binary systems, the fast mode term had more contributions to the ACF intensity compared to the slow mode term, *e.g.*, the I_f/I_s value of the LYS/PBS system (5 mg mL^{-1} at 37 °C) was 6.8 ± 3.2, the I_f/I_s value of the OVA/PBS system (5 mg mL^{-1} at 37 °C) was 1.9 ± 0.4, and the I_f/I_s value of the HA/PBS system (5 mg mL^{-1} at 37 °C) was 1.1 ± 0.1. These values also suggested that larger nano-colloids tended to have a smaller I_f/I_s and a higher intensity of the slow mode term. With regards to characteristic decay time, τ_{se} (slow relaxation-related decay time) was much larger and more variable than τ_f (diffusion-related decay time), *e.g.*, for the HA/PBS system (5 mg mL^{-1} at 37 °C), the value of τ_f was 42.0 ± 2.2 μs, whereas the value of τ_{se} was 1223 ± 692 μs. These standard deviation values, τ_f: 2.2 μs (relative standard deviation: 5%) *vs.* τ_{se}: 692 μs (relative standard deviation: 57%), indicated that diffusion coefficient was a more certain and predictable parameter compared to relaxation.

3.2. LYS/solvent and OVA/solvent binary systems

Fig. 2(a) and (b) showed the LYS diffusion coefficients at low (26 mM) and high (163 mM) ionic strengths. It was found that our measured values were similar (less than 10% different) to those measured using other techniques.[14] Also, at low ionic strength,

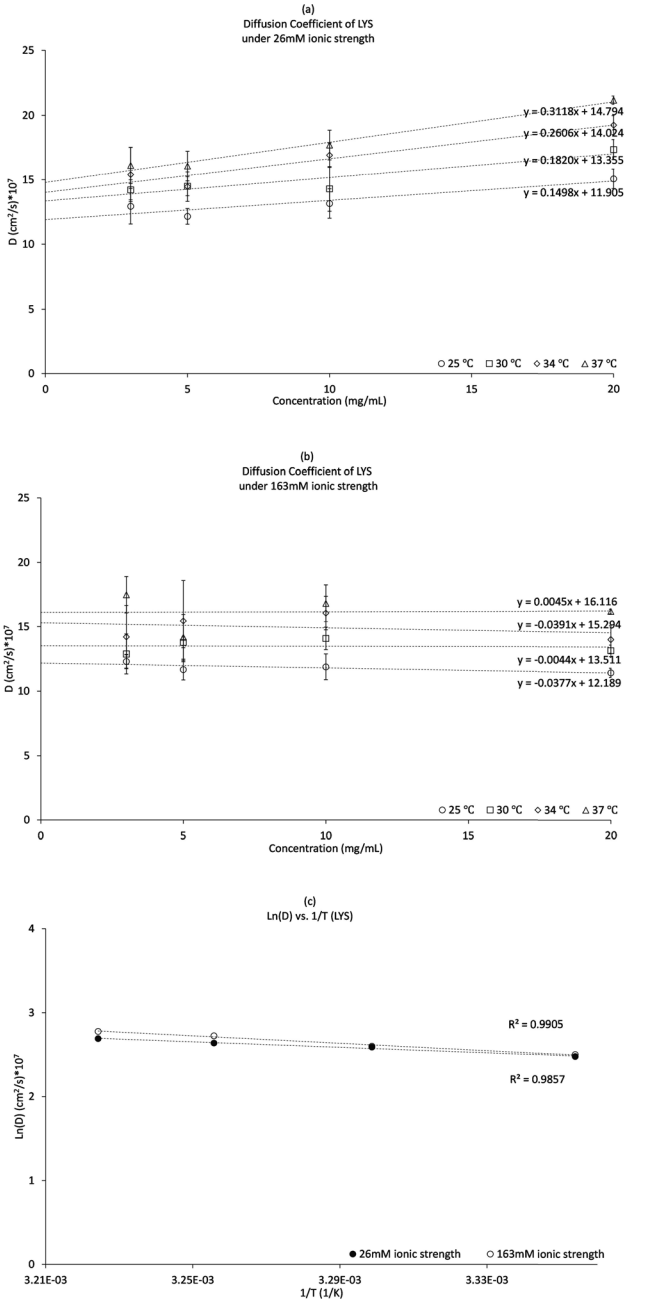

Fig. 2 Diffusion coefficients of LYS in binary systems (a) under 26 mM ionic strength; (b) under 163 mM ionic strength; (c) ln(*D*) *vs.* 1/*T*.

the correlation of diffusion coefficient and concentration could be fit by eqn (8).

$$D = D_0(1 + k_D C) \tag{8}$$

where D is the diffusion coefficient value measured by DLS, D_0 is the diffusion coefficient at infinitesimal concentration, and k_D is interaction parameter. As seen in Table 1, at low ionic strength, all k_D values were positive and significantly larger than 3.8 mL g^{-1} (a useful reference point related to the excluded volume term), denoting the existence of strong long-ranging repulsive protein–protein interaction in the diluted protein

Table 1 k_D values (in mL g^{-1}) at 26 mM ionic strength calculated from eqn 8

	LYS	OVA
25 °C	12.6	17.5
30 °C	13.6	21.4
34 °C	18.6	18.7
37 °C	21.1	19.6

systems.[19] Moreover, the repulsive interaction was highly likely to be contributed by electrostatic repulsion since other intermolecular forces such as van der Waals interaction, hydrophobic interaction, and hydrogen bond generally caused attractive interactions.[20] On the contrary, at high ionic strength, the k_D values was close to zero, indicating that intermolecular interaction was profoundly diminished by other ions in the solvent. It was also worthwhile to point out that the extrapolated diffusion coefficient values at infinitesimal concentration were similar (less than 10% in differences) between high and low ionic strengths, suggesting intermolecular interaction was extremely small at infinitely diluted state. Fig. 2(c) presented the relationship of ln(D) and 1/T, which followed the Arrhenius equation, as shown in eqn (9).

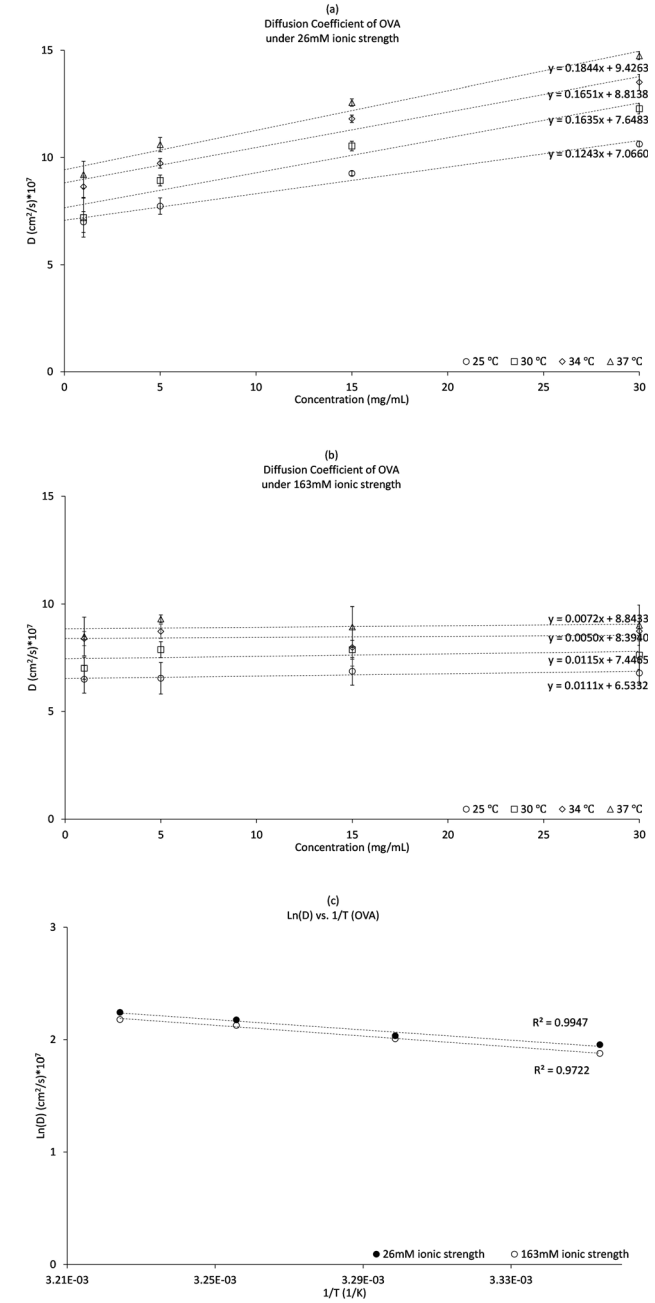

Fig. 3 Diffusion coefficients of OVA in binary systems (a) under 26 mM ionic strength; (b) under 163 mM ionic strength; (c) ln(D) *vs.* 1/T.

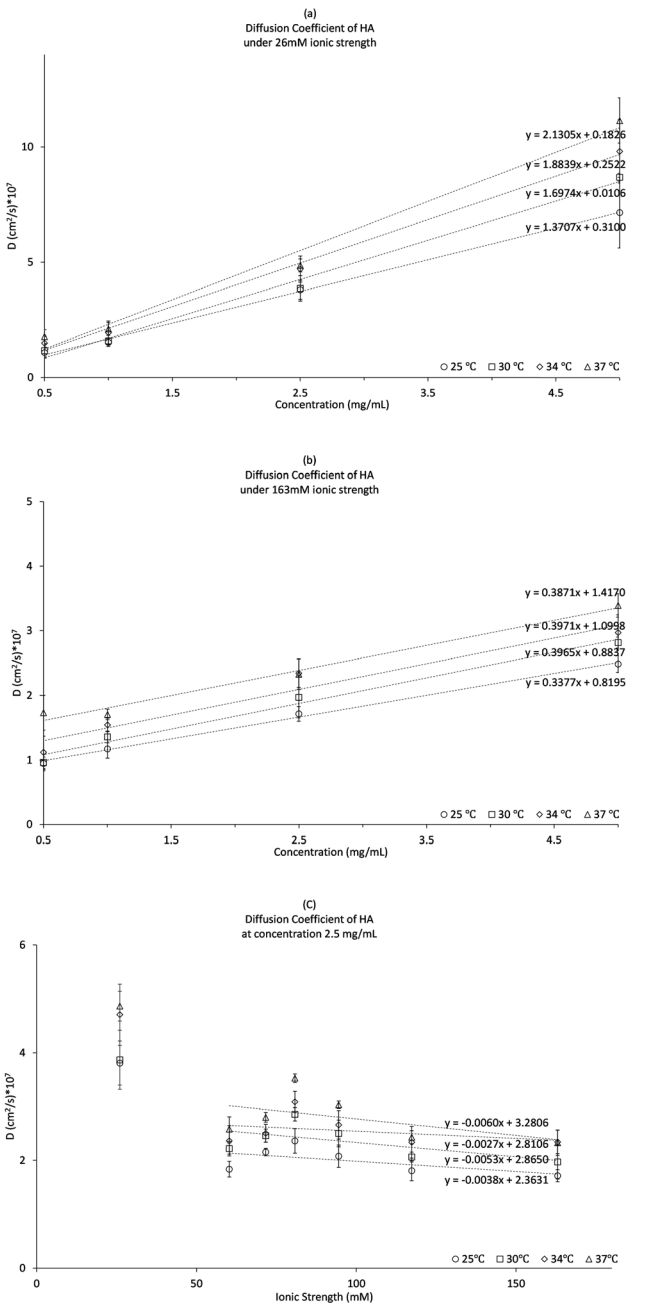

Fig. 4 Diffusion coefficients of HA in binary systems (a) under 26 mM ionic strength; (b) under 163 mM ionic strength; (c) *versus* ionic strength.

$$D = D^{\infty} \cdot \exp\left(-\frac{E}{RT}\right) \quad (9)$$

where D^{∞} is the infinite-temperature diffusivity, E is the activation energy, and R is the universal gas constant.

Fig. 3(a) and (b) showed the OVA diffusion coefficient values at low (26 mM) and high (163 mM) ionic strengths. The correlation of diffusion coefficient and concentration could also be fit by eqn (8). At low ionic strength, similar to LYS, the positive k_D values (listed in Table 1) indicated strong repulsive intermolecular interaction within the system. At high ionic strength, the k_D values were close to zero, which implied the dramatic weakening of intermolecular interaction. Compared to LYS, OVA was less diffusive, which was partially due to larger molecular volume/size. According to Wilke and Chang's equations, the diffusion coefficient was inversely proportional to solute molar volume at its boiling point to the order of 0.6.[21] For OVA, ln(D) *versus* $1/T$ also had an Arrhenius-type relationship, as shown in Fig. 3(c).

In addition, for the LYS (20 mg mL^{-1})/PBS and the OVA (30 mg mL^{-1})/PBS binary systems, the samples were still optically clear and the measured protein diffusion coefficients were equivalent to those measured in the lower concentrations, indicating that the ACFs were attained primarily from the singly scattered light. On the contrary, if there was an extensive presence of multiple scattering, which was a phenomenon that photons were re-scattered by neighboring particles before reaching the detector, then the more concentrated systems (*e.g.*, 20 or 30 mg mL^{-1}) tended to have a shorter decay time, a faster diffusion, as well as more signal randomness, compared to the less concentrated systems (*e.g.*, 1 or 3 mg mL^{-1}).[22]

3.3. HA/solvent binary systems

Fig. 4(a) and (b) showed that, for HA, diffusion coefficient and concentration also had a positive correlation. Further, compared to proteins, the diffusion coefficients of HA demonstrated a much stronger dependence on concentration (especially at 26 mM ionic strength), which might be due to the high density of negative charges on the HA chains. Even at high ionic strength (163 mM), the linear relationship between diffusion coefficient and concentration still existed, but the slope was much smaller compared to that at low ionic strength (26 mM). This effect of ionic strength on HA diffusion coefficients was also reported by other researchers.[23]

Fig. 4(c) presented HA diffusion coefficients at concentration 2.5 mg mL^{-1}. As seen, diffusion coefficients at 26 mM ionic strength were almost two-fold of those at modest and high ionic strengths, *i.e.*, at 25 °C, diffusion coefficient dropped from 3.8×10^{-7} cm^2 s^{-1} (at 26 mM ionic strength) to 1.8×10^{-7} cm^2 s^{-1} (at 60 mM ionic strength). Further, in the range of 60 mM and 163 mM, diffusion coefficients leveled out.

3.4. OVA/HA/solvent ternary systems

For OVA/HA/solvent ternary systems, Fig. 5 presented (D^1_{DLS} + D^2_{DLS}), equivalent to ($D_{11} + D_{22}$), under a series of concentration/ionic strength combinations. Overall, the diffusion coefficients

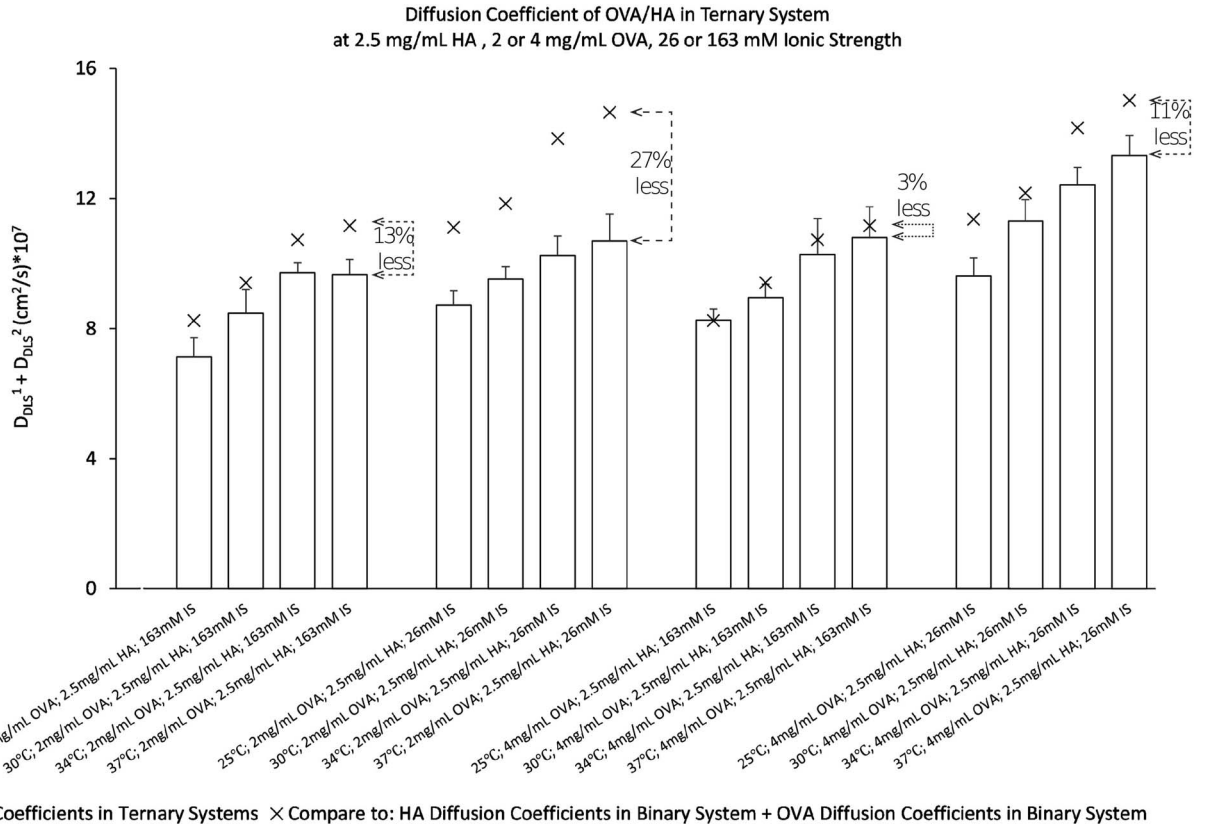

Fig. 5 Diffusion coefficients of OVA/HA/solvent ternary systems.

at low ionic strength (26 mM) were marginally higher compared to those at high (163 mM) ionic strength, which was due to the stronger repulsive intermolecular interactions for both OVA and HA molecules at low ionic strength. This explanation was further supported by the findings that the diffusion coefficients of more-concentrated systems (4 mg mL^{-1} OVA, 2.5 mg mL^{-1} HA) were slightly higher than those of less-concentrated systems (2 mg mL^{-1} OVA, 2.5 mg mL^{-1} HA), particularly at low ionic strength. It was also noted that diffusion coefficients in binary systems (*e.g.*, OVA/solvent and HA/solvent systems) and ternary systems changed in similar trends against ionic strength, concentration, and temperature. In addition, since OVA molecules diffused much faster than HA molecules in their corresponding binary systems, it was reasonable to extrapolate that, in ternary systems, D_{11} (for OVA) was larger than D_{22} (for HA). Further, Fig. 5 indicated that ($D^1_{DLS} + D^2_{DLS}$) (plotted as bars) were on average 12% lower than ($D_{OVA} + D_{HA}$) (plotted as signs "×"), where D_{OVA} and D_{HA} were separately measured from their corresponding HA/solvent and OVA/solvent binary systems. This discrepancy might be caused by the lowering of OVA diffusivity in presence of HA, which could be explained by two mechanisms suggested by Filippov *et al.*:[24] (1) high solvent viscosity: the interaction between HA and water molecules substantially lowered the mobility of water molecules and increased water "local-viscosity or micro-viscosity". The HA solution had high "macro-viscosity", which was mainly due to the formation of the HA network. However, the diffusion of OVA in the water phase was more related to water "micro-viscosity". In the presence of HA, water "micro-viscosity" increased because large quantities of water molecules bonded to HA and became less mobile, although water "micro-viscosity" should still be much lower than "macro-viscosity".[24] (2) volume fraction of HA in the solvent: OVA diffusion was hindered by the volume occupied by HA chains, which acted as mobile obstacles to exert steric effects. For a small mass fraction of HA (w_{HA}), the volume fraction of HA (φ_{HA}) could be calculated using eqn (10).

$$\varphi_{HA} \approx w_{HA} \frac{\nu_u \rho_s}{m_u} \quad (10)$$

where m_u is the molecular weight of a HA monomer (379 g mol^{-1}), ν_u is the estimated molecular volume of a HA monomer (estimated to be 395 $Å^3$),[24] ρ_s is the density of solvent (assumed to be equivalent to water density, 1 g mL^{-1}). For instance, at 2.5 mg mL^{-1} HA concentration, the volume fraction was around 0.26%.

3.5. LYS/HA/solvent ternary systems

For LYS/HA/solvent ternary systems, Fig. 6(a) and (b) presented ($D^1_{DLS} + D^2_{DLS}$) under a series of concentration/ionic strength combinations. As we observed, at low ionic strengths (*e.g.*, 26 mM), insoluble complex coacervates were formed in the systems containing 2 (or 4) mg mL^{-1} of LYS and 2.5 mg mL^{-1} of HA. Water *et al.* found that this coacervation was driven by the attractive electrostatic interaction between LYS and HA, and high ionic strength could effectively inhibit its formation.[25] Therefore, to prevent coacervate formation, diffusion coefficient characterization was undertaken at modest and high ionic

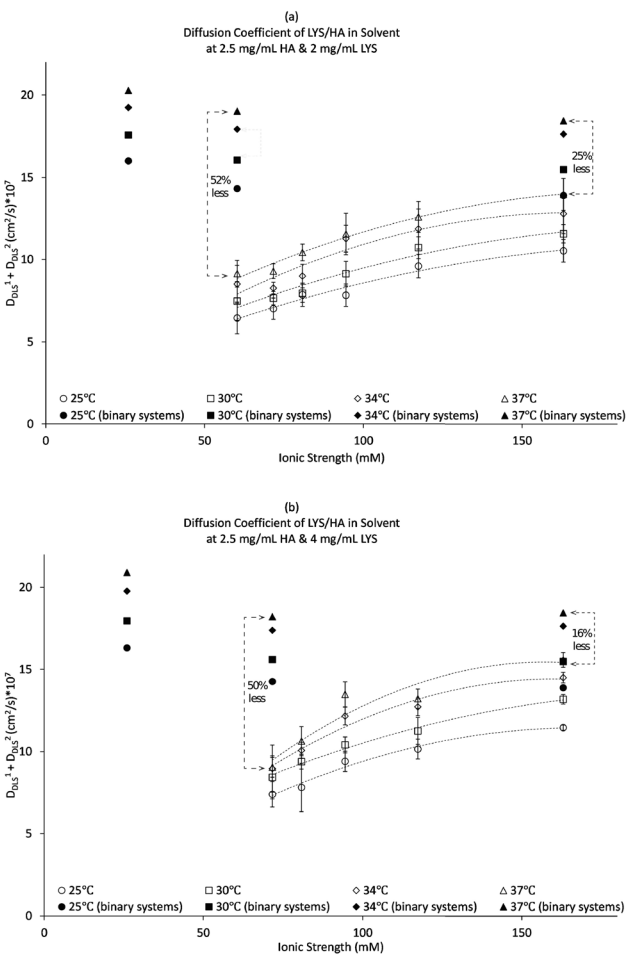

Fig. 6 Diffusion coefficients of LYS/HA/solvent ternary systems (a) at 2.5 mg mL^{-1} HA & 2 mg mL^{-1} LYS; (b) at 2.5 mg mL^{-1} HA & 4 mg mL^{-1} LYS.

strengths. As seen, as ionic strength became stronger, there was an increase of ($D^1_{DLS} + D^2_{DLS}$), *e.g.*, approximately a 50–70% increase from modest ionic strength (*e.g.*, 60 mM) to high ionic strength (*e.g.*, 163 mM).

Furthermore, the values of ($D^1_{DLS} + D^2_{DLS}$) were significantly lower than ($D_{LYS} + D_{HA}$), where D_{LYS} and D_{HA} were separately measured from their corresponding HA/solvent and LYS/solvent binary systems, *e.g.*, the ternary system was about 50% lower than the binary ones at modest ionic strength. It was also worthwhile pointing out that, for binary systems, a higher diffusion coefficient was observed at low (*e.g.*, 26 mM) ionic strength; oppositely, for ternary systems, a higher diffusion coefficient was observed at high (*e.g.*, 163 mM) ionic strength. This opposite trend of diffusion coefficients *versus* ionic strength was not observed in OVA binary and ternary systems, and could not be interpreted only using the two mechanisms listed in the Section of "OVA/HA/solvent ternary systems". We believed this opposite trend in LYS systems was mainly attributed to the "transient bound state" caused by the attractive intermolecular interaction between LYS and HA.[24,26] The surface electrostatic potential map at pH 7.4 (calculated by APBS/

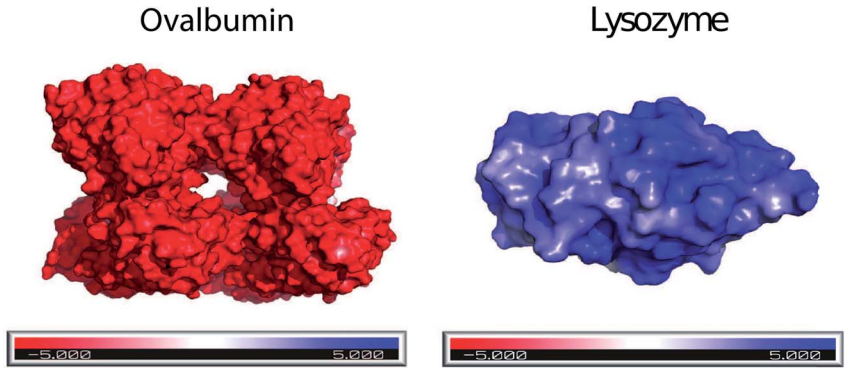

Fig. 7 Surface electrostatic potential map of LYS and OVA at pH 7.4.

Table 2 MD simulation of 1 LYS molecule and 8 HA monomers in 10 ps timeframe

Ionic strength (mM)	Electrostatic (kJ mol^{-1})	van der Waals (kJ mol^{-1})
45	−293.1 ± 128.2	−190.7 ± 47.8
80	−135.7 ± 84.6	−151.7 ± 73.6
150	−65.5 ± 69.1	−50.2 ± 45.3

PDB2PQR[27,28]) in Fig. 7 exhibited that the OVA (PDB code 1OVA[29]) surface had a high density of negatively charged patches, whereas the LYS (PDB code 1AKI[16]) surface was mostly covered by positively charged patches. HA is negatively charged, so the interaction between OVA and HA is repulsive, but the interaction between LYS and HA is attractive. Further, utilizing small-angle neutron scattering, Morfin *et al.* found that HA chains preferably stayed in "rod-like" elongated configuration in solvents, and multiple LYS molecules could reversibly attach to the HA chain.[30] Unfortunately, this dynamic exchange of LYS molecules between "bound state" and "free state" might be too transient to be detected by DLS, and the apparent diffusion coefficients provided by DLS was an interplay of "bound" and "free" states.

The interaction between LYS and HA was also studied using MD simulation. Table 2 listed the van der Waals and electrostatic interactions between LYS and HA molecules within the 10 ps simulation timeframe. As seen, as ionic strength increased, the attractive electrostatic interaction dropped drastically, *e.g.*, −293.1 kJ mol^{-1} (45 mM) *vs.* −65.5 kJ mol^{-1} (150 mM). In addition, with the higher ionic strength, perhaps due to the further distance between LYS and HA molecules, van der Waals interaction also became smaller. Overall, these simulation results, along with the DLS results, both revealed that higher ionic strength profoundly weakened the interaction between LYS and HA.

4. Conclusion

This study showed that by using DLS it was possible to characterize the diffusion coefficients of multiple diluted protein and HA systems. For LYS/solvent and OVA/solvent binary systems, the diffusion coefficient was linearly correlated to protein concentration at low ionic strength (26 mM) but became independent of protein concentration at high ionic strength (163 mM). For HA/solvent binary systems, the positive linear correlation between diffusion coefficient and concentration existed at both low and high ionic strengths, but the slope at high ionic strength was much flatter compared to that at low ionic strength.

For the ternary systems, DLS provided the sum of two eigenvalues of the diffusion coefficient matrix. For OVA/HA/solvent systems, the sum of two eigenvalues (D^1_{DLS} + D^2_{DLS}) were slightly lower compared to (D_{OVA} + D_{HA}) obtained from their binary systems. This difference might be due to the increased solvent viscosity and the steric effect of HA as a "mobile obstacle". Oppositely, for LYS/HA/solvent systems, (D^1_{DLS} + D^2_{DLS}) was significantly lower as compared to (D_{LYS} + D_{HA}) obtained from their binary systems, and diffusion coefficients in binary and ternary systems presented an opposite trend to ionic strength change. The DLS results, along with the MD simulation results, suggested the existence of strong attractive intermolecular interaction between LYS and HA molecules, especially at low ionic strength.

Conflicts of interest

The authors declare that they have no known competing financial interests.

References

1 T. C. Laurent and J. R. E. Fraser, *Hyaluronan*, 1992, **6**(7), 2397–2404.
2 J. R. E. Fraser, T. C. Laurent and U. B. G. Laurent, Hyaluronan: its nature, distribution, functions and turnover, *J. Intern. Med.*, 1997, **242**(1), 27–33.
3 H. Saari, Y. T. Konttinen, C. Friman and T. Sorsa, Differential effects of reactive oxygen species on native synovial fluid and purified human umbilical cord hyaluronate, *Inflammation*, 1993, **17**(4), 403–415.
4 H. M. Kinnunen and R. J. Mrsny, Improving the outcomes of biopharmaceutical delivery *via* the subcutaneous route by

understanding the chemical, physical and physiological properties of the subcutaneous injection site, *J. Controlled Release*, 2014, **182**, 22–32.

5 J. Y. Song, N. R. Larson, S. Thati, I. Torres-Vazquez, N. Martinez-Rivera, N. J. Subelzu, *et al.*, Glatiramer acetate persists at the injection site and draining lymph nodes *via* electrostatically-induced aggregation, *J. Controlled Release*, 2019, **293**, 36–47.

6 S. Bhattacharjee, DLS and zeta potential – What they are and what they are not?, *J. Controlled Release*, 2016, **235**, 337–351.

7 J. Stetefeld, S. A. McKenna and T. R. Patel, Dynamic light scattering: a practical guide and applications in biomedical sciences, *Biophys. Rev.*, 2016, **8**(4), 409–427.

8 B. Das, B. Maitra, S. M. Mercer, M. Everist and D. G. Leaist, A comparison of diffusion coefficients for ternary mixed micelle solutions measured by macroscopic gradient and dynamic light scattering techniques, *Phys. Chem. Chem. Phys.*, 2008, **10**(21), 3083–3092.

9 A. Heller, C. Giraudet, Z. A. Makrodimitri, M. S. H. Fleys, J. Chen, G. P. van der Laan, *et al.*, Diffusivities of Ternary Mixtures of n-Alkanes with Dissolved Gases by Dynamic Light Scattering, *J. Phys. Chem. B*, 2016, **120**(41), 10808–10823.

10 A. Bardow, On the interpretation of ternary diffusion measurements in low-molecular weight fluids by dynamic light scattering, *Fluid Phase Equilib.*, 2007, **251**(2), 121–127.

11 P. A. Hassan, S. Rana and G. Verma, Making Sense of Brownian Motion: Colloid Characterization by Dynamic Light Scattering, *Langmuir*, 2015, **31**(1), 3–12.

12 A. Maleki, A.-L. Kjøniksen and B. Nyström, Effect of pH on the Behavior of Hyaluronic Acid in Dilute and Semidilute Aqueous Solutions, *Macromol. Symp.*, 2008, **274**(1), 131–140.

13 A. Heller, T. M. Koller, M. H. Rausch, M. S. H. Fleys, A. N. R. Bos, G. P. van der Laan, *et al.*, Simultaneous Determination of Thermal and Mutual Diffusivity of Binary Mixtures of n-Octacosane with Carbon Monoxide, Hydrogen, and Water by Dynamic Light Scattering, *J. Phys. Chem. B*, 2014, **118**(14), 3981–3990.

14 M. Yu, T. C. Silva, A. van Opstal, S. Romeijn, H. A. Every, W. Jiskoot, *et al.*, The Investigation of Protein Diffusion *via* H-Cell Microfluidics, *Biophys. J.*, 2019, **116**(4), 595–609.

15 M. J. Abraham, T. Murtola, R. Schulz, S. Páll, J. C. Smith, B. Hess, *et al.*, GROMACS: High performance molecular simulations through multi-level parallelism from laptops to supercomputers, *SoftwareX*, 2015, **1–2**, 19–25.

16 P. J. Artymiuk, C. C. F. Blake, D. W. Rice and K. S. Wilson, The structures of the monoclinic and orthorhombic forms of hen egg-white lysozyme at 6 Å resolution, *Acta Crystallogr., Sect. B: Struct. Crystallogr. Cryst. Chem.*, 1982, **38**(3), 778–783.

17 W. L. Jorgensen and J. Tirado-Rives, Potential energy functions for atomic-level simulations of water and organic and biomolecular systems, *Proc. Natl. Acad. Sci. U. S. A.*, 2005, **102**(19), 6665–6670.

18 L. S. Dodda, I. Cabeza de Vaca, J. Tirado-Rives and W. L. Jorgensen, LigParGen web server: an automatic OPLS-AA parameter generator for organic ligands, *Nucleic Acids Res.*, 2017, **45**(W1), W331–W336.

19 D. Roberts, R. Keeling, M. Tracka, C. F. van der Walle, S. Uddin, J. Warwicker, *et al.*, Specific Ion and Buffer Effects on Protein–Protein Interactions of a Monoclonal Antibody, *Mol. Pharm.*, 2015, **12**(1), 179–193.

20 M. Hofmann and H. Gieseler, Predictive Screening Tools Used in High-Concentration Protein Formulation Development, *J. Pharm. Sci.*, 2018, **107**(3), 772–777.

21 C. R. Wilke and P. Chang, Correlation of diffusion coefficients in dilute solutions, *AIChE J.*, 1955, **1**(2), 264–270.

22 R. Ragheb and U. Nobbmann, Multiple scattering effects on intercept, size, polydispersity index, and intensity for parallel (VV) and perpendicular (VH) polarization detection in photon correlation spectroscopy, *Sci. Rep.*, 2020, **10**(1), 21768.

23 F. Horkay, P. J. Basser, D. J. Londono, A.-M. Hecht and E. Geissler, Ions in hyaluronic acid solutions, *J. Chem. Phys.*, 2009, **131**(18), 184902.

24 A. Filippov, M. Artamonova, M. Rudakova, R. Gimatdinov and V. Skirda, Self-diffusion in a hyaluronic acid–albumin–water system as studied by NMR, *Magn. Reson. Chem.*, 2012, **50**(2), 114–119.

25 J. J. Water, M. M. Schack, A. Velazquez-Campoy, M. J. Maltesen, M. van de Weert and L. Jorgensen, Complex coacervates of hyaluronic acid and lysozyme: Effect on protein structure and physical stability, *Eur. J. Pharm. Biopharm.*, 2014, **88**(2), 325–331.

26 J. Bernstein and J. Fricks, Analysis of single particle diffusion with transient binding using particle filtering, *J. Theor. Biol.*, 2016, **401**, 109–121.

27 N. A. Baker, D. Sept, S. Joseph, M. J. Holst and J. A. McCammon, Electrostatics of nanosystems: Application to microtubules and the ribosome, *Proc. Natl. Acad. Sci. U.S.A.*, 2001, **98**(18), 10037–10041.

28 T. J. Dolinsky, J. E. Nielsen, J. A. McCammon and N. A. Baker, PDB2PQR: an automated pipeline for the setup of Poisson-Boltzmann electrostatics calculations, *Nucleic Acids Res.*, 2004, **32**(Web Server issue), W665–W667.

29 P. E. Stein, A. G. Leslie, J. T. Finch and R. W. Carrell, Crystal structure of uncleaved ovalbumin at 1.95 A resolution, *J. Mol. Biol.*, 1991, **221**(3), 941–959.

30 I. Morfin, E. Buhler, F. Cousin, I. Grillo and F. Boué, Rodlike Complexes of a Polyelectrolyte (Hyaluronan) and a Protein (Lysozyme) Observed by SANS, *Biomacromolecules*, 2011, **12**(4), 859–870.